EGYPTIAN PHARMACEUTICAL JOURNAL EPJ

Original article **257**

Untargeted metabolomic, network pharmacology, and molecular docking of Sunda porcupine's quills (*Hystrix javanica*, F. Cuvier 1823) extract for wound healing

Budiman Muhamad A.[1], Sari Shinta D. P.[2], Elfirta Rizki R.[3], Masrukhin[4], Nugroho Herjuno A.[5], Farida Wartika R.[6], Amalia Raden L. R.[7], Ferdian Pamungkas R.[8.]

[1]Faculty of Medicine, Universitas Muhammadiyah Prof. DR. HAMKA, Jl. Raden Fatah No.01, RT.002/RW.006, Parung Serab, Kec. Ciledug, Tangerang, Banten 13460, Indonesia,[2]Faculty of Medicine, Universitas Muhammadiyah Prof. DR. HAMKA, Jl. Raden Fatah No.01, RT.002/RW.006, Parung Serab, Kec. Ciledug, Tangerang, Banten 13460, Indonesia, [3]Research Centre for Applied Microbiology, National Research and Innovation Agency (BRIN). Jl. Raya Jakarta-Bogor Km 46. Cibinong, Bogor, West Java 16911, Indonesia, [4]Research Centre for Biosystematics and Evolution, National Research and Innovation Agency (BRIN). Jl. Raya Jakarta-Bogor Km 46. Cibinong, Bogor, West Java 16911, Indonesia, [5]Research Centre for Applied Microbiology, National Research and Innovation Agency (BRIN). Jl. Raya Jakarta-Bogor Km 46. Cibinong, Bogor, West Java 16911, Indonesia, [6]Research Centre for Applied Zoology, National Research and Innovation Agency (BRIN). Jl. Raya Jakarta-Bogor Km 46. Cibinong, Bogor, West Java 16911, Indonesia, [7]Research Centre for Applied Zoology, National Research and Innovation Agency (BRIN). Jl. Raya Jakarta-Bogor Km 46. Cibinong, Bogor, West Java 16911, Indonesia, [8]Research Centre for Applied Zoology, National Research and Innovation Agency (BRIN). Jl. Raya Jakarta-Bogor Km 46. Cibinong, Bogor, West Java 16911, Indonesia

Corresponding Author: Ferdian Pamungkas R., M.Sc., *Jl. Raya Jakarta-Bogor Km 46. Cibinong, Bogor, West Java 16911, Indonesia, E-mail: pamu003@brin.go.id, Phone numbers +6285219947997*

Received: 09 October 2024
Revised: 18 December 2024
Accepted: 19 December 2024
Published: 23 February 2025

Egyptian Pharmaceutical Journal 2025, 24: 257-273

Background

The Sunda porcupine's quills (*Hystrix javanica*, F. Cuvier 1823) have been traditionally used in Indonesian medicine for their pain-relieving properties, particularly toothaches. Additionally, Sunda porcupine is known for its skin's impressive wound healing abilities, leading to speculating that the quills may also possess wound healing potential.

Objective

The objective of this study is to identify bioactive components in Sunda porcupine's quills extract using UPLC-MS/MS and GC-MS, and to explore the wound healing potential of these compounds through network pharmacology and molecular docking analysis.

Materials and methods

Sunda porcupine's quills were collected, dried at 50 °C, and extracted using 70% ethanol *via* maceration. The extract underwent metabolomic profiling using GC-MS and UPLC-MS/MS, with data analyzed through NIST-11 and databases such as ChemSpider and MassBank. Target proteins associated with skin wound healing were sourced from GeneCards, CTD, and PubMed, while the target proteins of Sunda porcupine's quills active compounds were identified using SwissTargetPrediction and SEA server. Protein-protein interactions were analyzed with STRING, followed by enrichment analysis *via* DAVID. Molecular docking was performed using AutoDock-4.2, while drug-likeliness and toxicity were assessed using SwissADME and Protox II. Results were visualized in 2D and 3D using Discovery Studio Visualizer.

Results and conclusion

Thirty two compounds were identified in the Sunda porcupine's quills extract through UPLC-MS/MS and GC-MS analysis. Network pharmacology revealed that the extract targeted vital inflammatory markers, including IL6, IL1β, and TNFα, which are involved in both skin wound healing and the active compounds of the Sunda porcupine's quills extract. Molecular docking analysis showed that compounds such as resolvin-D2, hypoxanthine, carnitine, indoline, pentanedioic acid 2,4-dimethyl-dimethyl ester, (11α,13E,15S)-11,15-dihydroxy-9-oxoprost-13-en-1-oate, and 1-dodecanol displayed a potential inhibitory effect on proinflammatory cytokines (IL6, IL1β, and TNFα) and on PPARγ, which plays a role in cell proliferation during the wound healing process.

Keywords: ethnomedicine, Indonesian fauna, in silico, natural product profiling.
Egypt Pharmaceut J 24:0–0

Introduction

Skin acts as the body's first line of defense against pathogens and harmful substances, and damage to the skin, such as from wounds, can disrupt this protective barrier. Wound healing is a complex, multi-stage process involving cell migration, proliferation, and inflammatory responses [1]. Traditional medicines derived from natural products have long been used to accelerate wound healing, especially in cases of delayed recovery [2]. These natural products often contain various bioactive compounds that interact with various biological pathways to support the healing process [3].

Ethnomedicine has played a significant role in wound management in many cultures, with remedies passed down through generations. In Indonesia, communities use various animal-derived products for their medicinal properties. Notably, the Sunda porcupine (*Hystrix javanica*) is believed to possess healing properties [4-5]. Its quills have been traditionally used by locals in the Kalimantan and Dayak communities to treat conditions such as acne, toothaches, and back pain [6]. Similar practices have been reported in Malaysia, where porcupine quills are used to treat breathlessness and asthma [7]. Recent studies have shown that the extract from Sunda porcupine's quills has antimicrobial and antioxidant properties, particularly against pathogens like *Staphylococcus aureus* and *Bacillus subtilis* [8].

Despite these traditional uses, the specific bioactive compounds in Sunda porcupine's quills that contribute to wound healing remain unidentified. This study aims to identify bioactive compounds in Sunda porcupine's quills using UPLC-MS/MS and GC-MS. By employing computational tools such as network pharmacology analysis and molecular docking, this study also aims to

uncover the potential of these bioactive compounds in the wound healing process. This research can provide a scientific basis for the medicinal use of Sunda porcupine's quills and contribute to the growing body of knowledge on animal-derived ethnomedicine.

Materials and methods

Samples

Sunda porcupine's quills were collected from a physiological study approved by the Indonesian Institute of Sciences (protocol number B-15897/IPH/KS/02/04/XII/2019).

Extraction

The cleaned Sunda porcupine's quills were dried at 50 °C and grounded to a size of 60 mesh to produce simplicia powder. The quills simplicia were then extracted using 70% ethanol with a simplicia to solvent ratio of 1:30 through the maceration method. Subsequently, the mixture of solvent-simplicia was filtered using filter paper. After that, the filtrate solution was heated by a rotary evaporator at 40 °C to remove all solvent and obtain the crude extract. It was then stored at 4 °C for future use.

Metabolomic profiling

Metabolomic profiling was conducted using GC-MS and UPLC-MS/MS. The extract was dissolved in methanol to the concentration 1000 µg/mL, filtered, and injected separately into a GC-MS and UPLC-MS/MS instrument. The GC-MS instrument was set using an Rtx-5MS column (5% diphenyl: 95% dimethyl-polysiloxane with 30 m length and 0.25 mm diameter), temperature set at 200 °C, the ion source at 230 °C, the interphase at 280 °C, and splitless injection mode. The oven temperature program was initiated at 60 °C , increased to 150 °C at a rate of 10 °C/minute, and held for 3 minutes. The GC-MS chromatogram was analyzed using the NIST-11 library.

The UPLC-MS/MS was analyzed using a mobile phase consisting of 5 mM ammonium formate in H_2O and 0.05% formic acid in acetonitrile, with a flow rate of 0.20 mL/min and a column temperature of 50℃. A C18 HSS T3 1.8 µm column and QTOF detector with electrospray ionization (ESI) and positive ion mode were used. Chromatogram analysis was conducted using Masslynx software. Using the software, the first analysis was conducted to MS1 to identify the molecular formula and fit confidence of the compounds. In this state, the compound should have an intact structure since the analysis using low energy. After that, the analysis was performed using MS2 with higher energy. In this step, the structure of each identified compound will be fragmented into daughter ions which can be a specific marker to confirm the structure of the compounds. The molecular formulas and spectra were compared with databases such as ChemSpider, PubChem, MassBank, HMDB, and NIST [8-9]. Compounds will be categorized as "unknown" if their fit confidence (fit conf) values are below 75% based on MassLynx analysis or if their molecular formulas cannot be identified in the ChemSpider database. Compounds will be classified as "suspected" if they have fit conf values greater than 75% and their molecular formulas are identified using ChemSpider, but they lack sufficient matching daughter ions data between MassLynx readings and the MassBank database. Compounds will be grouped as "confirmed" if they exhibit fit conf values exceeding 75%, have molecular formulas identified in ChemSpider, and show matching daughter ions data between MassLynx readings and MassBank database. Compounds in the suspected and confirmed categories will be included in subsequent analysis, if their fit conf values above 75% and identification in ChemSpider suggest a high probability of accurate identification. The inclusion of these two compound categories was also intended to expand the diversity of compounds analyzed in network pharmacology and molecular docking studies. This approach aims to wider exploration of the potential of Sunda porcupine's quills for promoting skin wound healing .

Constructing target proteins associated with skin wound healing and target proteins of Sunda porcupine's quills compounds

Skin wound healing was obtained from the GeneCards (https://www.genecards.org), comparative toxicogenomic database (CTD) (https://ctdbase.org), and PubMed databases by using "skin wound healing ", "protein coding", and "wound and injuries" keywords (PMID: 36230913, PMID: 34313846, PMID: 34193119, PMID: 33182690, PMID: 31275545, PMID: 34945243). Meanwhile, target proteins of Sunda porcupine's quills active compound were collected using SwissTargetPrediction (http://www.swisstargetprediction.ch), SEA server (https://sea.bkslab.org/), and CTD (https://ctdbase.org/). On the SwissTargetPrediction and SEA server database, the SMILES line entries of the active compounds were filled in for data collection. In the CTD database, each active compound was filled in a chemical keyword search. Both sets of target proteins associated with skin wound healing and target proteins of Sunda porcupine's quills active compound were intersected using a Venn diagram to identify common protein targets [9-10]. These intersected proteins were then constructed through protein-protein interaction (PPI) analysis.

Protein-protein interaction (PPI) and enrichment analysis

Potential protein targets related to skin wound healing were analyzed using the STRING database (version 12) with "*Homo sapiens*" as the organism and an interaction score of ≥ 0.7 as a high confidence value. The PPI network was visualized in Cytoscape, and node analysis was based on degree values [10, 11]. Gene ontology (GO) and Kyoto Encyclopedia of Genes and Genomes (KEGG) pathway enrichment observations were performed using the DAVID database (https://david.ncifcrf.gov/home.jsp), focusing on biological process (BP), cellular component (CC), and molecular functions (MF). The top ten KEGG pathways ($p<0.05$) were selected and visualized.

Molecular docking

The active compounds of Sunda porcupine's quills extract selected from SwissTargetPredicion, SEA, and CTD were reconstructed using ChemSketch, while the target proteins associated with skin wound healing from PPI were downloaded from the RCSB database (https://www.rcsb.org/) as receptors in molecular docking study. Predicted Lipinski's rule of five was applied to assess drug-likeliness *via* SwissADME (http://www.swissadme.ch/), and predicted toxicity class was analyzed *via* Protox (https://tox-new.charite.de/protox_II/). Molecular docking was performed using Autodock-4.2 which set the grid box comprising 24x24x24 points spaced by 0.375 Å, the Lamarckian Genetic Algorithm (LGA) of 100 runs, the population size of 150, the mutation rate of 0.02, and the crossover rate of 0.80. The lowest binding energy (ΔG) ligand conformation was analyzed in 2D and 3D with Discovery Studio Visualizer [11].

Results

Metabolomic analysis using GC-MS and UPLC-MS/MS

The compounds in Sunda porcupine's quills extract were identified through a metabolomic study using GC-MS and UPLC-MS/MS. The GC-MS chromatogram is presented in Fig. 1, while the UPLC-MS/MS chromatogram is shown in Fig. 2. A total of 7 compounds were identified from the GC-MS analysis (Table 1). While most of the detected peaks on the GC-MS chromatogram were successfully matched with compounds in the databases, two peaks at 14 minutes and between 36 and 37 minutes did not correspond to any known compounds, suggesting the presence of potentially novel or less-characterized bioactive substances. These unidentified peaks warrant further investigation to determine their chemical structure and biological relevance.

In addition, 25 compounds were identified using UPLC-MS/MS, with 17 compounds suspected and 8 compounds confirmed (Table 2). From the chromatogram analysis, 39 distinct peaks were observed, with several corresponding to unknown compounds. Combined with the result from GC-MS, a total of 32 compounds were identified. These compounds were screened through network pharmacology to identify those related to wound healing receptors, while the unknown peaks suggest the potential presence of novel bioactive compounds requiring further investigation.

Intersection target proteins associated with skin wound healing and target proteins of Sunda porcupine's quills compounds

Three databases (GeneCards, PMID, and CTD) were used to get 77 target proteins associated with skin wound healing of 16774 compounds after removing duplicate values (Fig. 3a). Then, 29 targets were taken after removing duplicates and the intersecting the three databases using a Venn diagram. The intersection between the target proteins of Sunda porcupine's quills active compound and target proteins associated with skin wound healing was obtained 41 potential targets and is depicted in Fig. 3b. Potential targets were submitted to the STRING database with "*Homo sapiens*" as the organism to obtain protein interaction networks, visualizing pathways between nodes and edges. After the high confidence score was adjusted, the potential target network data was imported into Cytoscape version 3.10.0. The PPI network was obtained with 33 potential targets selected based on degree level (□3). Key potential targets included TNFα, IL6, IL1β, IL10, CXCL8, MMP9, TGFB1, PTGS2, CCL2, IFNγ, IL4, MMP3, IL1A, PPARγ, TIMP1, F3, HIF1A, LEP, PLAU, PDGFRA, RHOA, MAPK14, ERBB2, F2, TGFα, KNG1, PLAT, SIRT1, CD36, CPB2, F2R, ERBB3, and FGFR2 (Fig. 3c). The compound-target network of Sunda porcupine's quills extract targeted to PPI wound healing of the skin are shown in Fig. 4.

GO and KEGG enrichment analysis

A total of 41 potential targets were submitted to the DAVID database for Gene Ontology (GO) and KEGG enrichment. Among all potential targets, 261 biological processes (BP), 16 cellular components (CC), and 20 molecular functions (MF) were identified with a p-value < 0.05. The term "top three BP" refers to processes such as cell response to lipopolysaccharide (a component of the outer membrane of Gram-negative bacteria), positive regulation of cell population proliferation, and positive regulation of gene expression. The top three CC terms relate to the cellular locations of gene products, specifically the extracellular space, extracellular region, and cell survival. The top three of MF terms indicate cytokine activity, growth factor activity, and protein binding activity. Pathways associated with BP, CC, and MP are shown in Fig. 5. KEGG analysis identified 10 signaling pathways related to potential targets ($p<0.05$), including pathways in cancer and the IL-17 signaling pathway. The top 10 pathways with KEGG enrichment values are shown in Fig. 6.

Molecular docking

Molecular docking was conducted on corecompounds in Sunda porcupine's quills extract targeting IL6 (PDB ID: 1ALU), IL1β (PDB ID: 5R86), TNFα (PDB ID: 2AZ5), PPARγ (PDB ID: 2PRG) as receptor targets. ResolvinD2, hypoxanthine, carnitine, indoline, (11α,13E,15S)-11,15-dihydroxy-9-oxoprost-13-en-1-oate, 1-dodecanol, and pentanedioic acid, 2,4-dimethyl-, dimethyl ester adhered to Lipinski's rule of five based on drug-likeliness with zero violations. Most compounds were predicted to fall into toxicity categories III, IV, V, and VI (Table 3). The four receptors had a resolution of less than 2.5 Å and were in a stable state based on Ramachandran plot, with less than 15% occupancy in the disallowed region (Fig. 7). The binding pocket center (x, y, z) performed for IL6, IL1β, TNFα, and PPARγ were (-7.854, -12.939, -0.226), (42.035, 26.718, 65.929), (-9.181, 67.363, 20.045), and (50.806, -38.214, 19.575), respectively. The docking process was validated by docking the natural ligand and comparing the Root Mean Square Deviation (RMSD) values. An RMSD value of less than 2 Å was considered valid (Fig. 8). The molecular docking results are presented in Table 4, while the 2D and 3D interactions illustrated in Fig. 9-12.

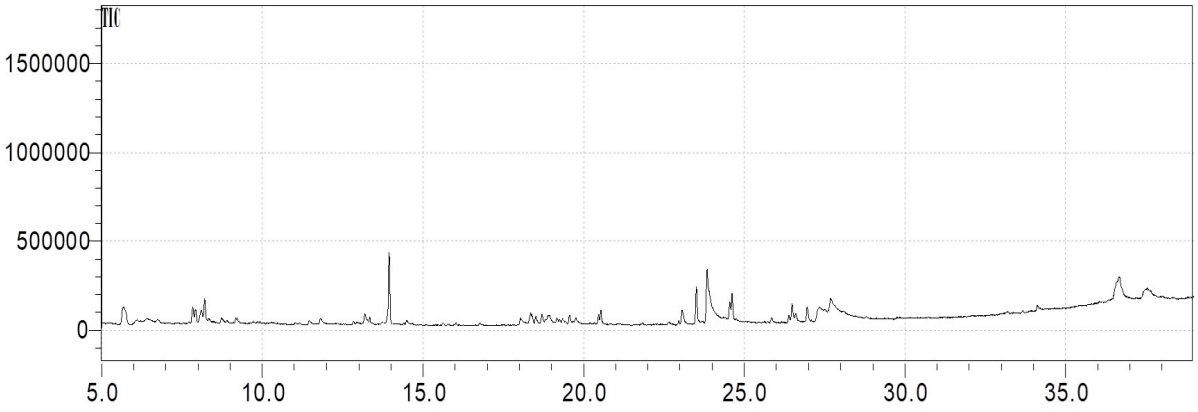

Fig. 1 GC-MS chromatogram of Sunda porcupine's quills extract.

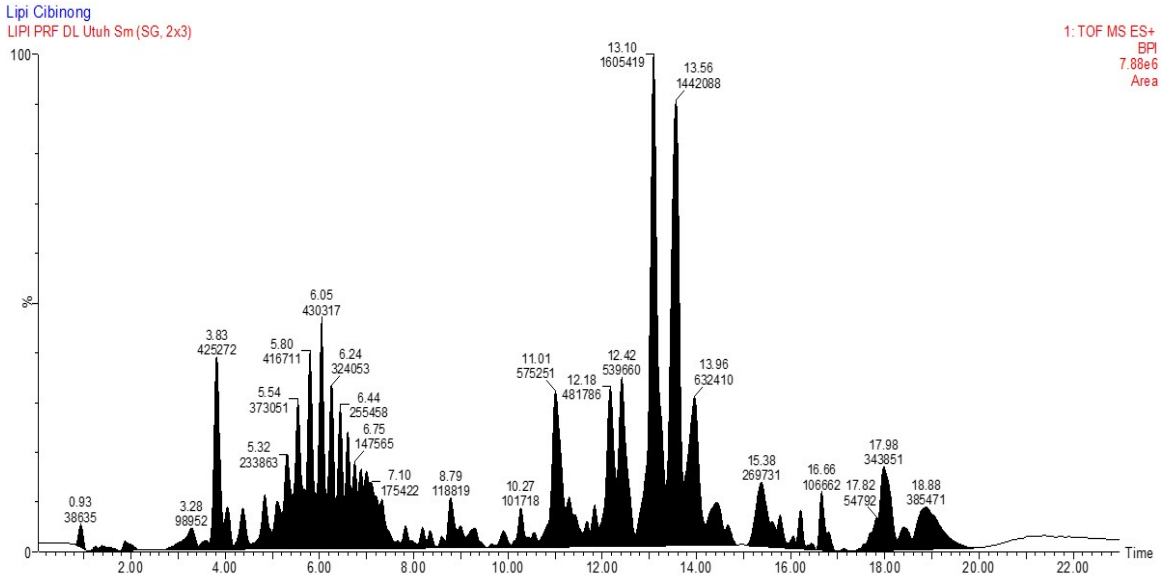

Fig. 2 UPLC-MS/MS chromatogram of Sunda porcupine's quills extract

Table 1 Identified compounds from Sunda porcupine's quills extract by GC-MS.

Retention Time	Name	Relative abundance (%)	Molecular Formula	Compound Class	Similarity (%)
7.924	1-Dodecanol	**5.033**	$C_{12}H_{26}O$	Alcohol	94
8.200	Pentanedioic acid, 2,4-dimethyl-, dimethyl ester	5.674	$C_9H_{16}O_4$	Carboxylic acid	92
23.064	Hexadecanoic acid, methyl ester	5.821	$C_{17}H_{34}O_2$	Ester	93
23.505	Benzenepropanoic acid, 3,5-bis(1,1-dimethylethyl)-4-hydroxy-, methyl ester	10.487	$C_{18}H_{28}O_3$	Ester	90
23.843	l-(+)-Ascorbic acid 2,6-dihexadecanoate	32.694	$C_{38}H_{68}O_8$	Ester	86
24.547	5-Methyl-1-phenylbicyclo[3.2.0]heptane	13.242	$C_{14}H_{18}$	Unknown	68
26.955	Methyl stearate	4.926	$C_{19}H_{38}O_2$	Ester	93

Table 2 Identified compounds from Sunda porcupine's quills extract by UPLC-MS/MS.

RT (min)	Relative abundance (%)	MF ML [M+H]+	Fit Conf (%)	Molecular weight [M+H]+ m/z	Confirmed daughter ions (m/z)	Compound name	Compound group	Status
0.93	0.32	$C_3H_8N_4OCl$	84.46	151.0365	-	Unknown	-	-
1.232	0.055	$C_7H_{16}NO_3$	100	162.1137	112.8971, 84.0820, 70.7372, 57.0010	Carnitine	Amino acid derivative	confirmed
1.386	0.18	$C_{13}H_{20}N_5$	49.56	246.1712	-	Unknown	-	-
1.872	0.242	$C_5H_5N_4O$	99.74	137.0473	136.063; 110.0717;	Hypoxanthine	Purine	confirmed
3.278	0.82	$C_8H_{10}N$	100	120.082	77.0383; 91.0541; 103.0541	Indoline	Indoles	confirmed
3.587	0.196	$C_{11}H_{16}NO_{10}$	81.06	322.0775	-	N-[3-Carboxy-2-(carboxymethyl)-2-hydroxypropanoyl]-L-glutamic acid	Amino acid derivative	suspected
3.826	3.522	$C_{12}H_{16}N_3O$	98.39	218.1296	56.0501, 97.0766, 159.0925	Noramidopyrine	Pyrazole	confirmed
4.044	0.756	$C_{11}H_{10}NO_2$	100	188.0719	-	(2E)-3-(1H-Indol-3-yl)acrylic acid	Indoles	suspected
4.374	0.892	$C_{12}H_{24}NO_4$	97.57	246.1714	-	5-Methyl-3-({[(2-methyl-2-propanyl)oxy]carbonyl}amino)hexanoic acid	Amino acid derivative	suspected
4.839	1.292	$C_{14}H_{23}N_2O$	99.98	235.1818	136.0765; 193.0996; 114.0668; 70.0658	Angustifoline	Alkaloid	confirmed
5.098	1.032	$C_{20}H_{43}O_{11}$	98.88	459.2809	-	3,6,9,12,15,18,21,24,27-Nonaoxanonacosane-1,29-diol	Alcohol	suspected
5.324	1.937	$C_{22}H_{47}O_{12}$	99.66	503.3079	-	3,6,9,12,15,18,21,24,27,30-Decaoxadotriacontane-1,32-diol	Alcohol	Suspected
5.542	3.09	$C_{24}H_{51}O_{13}$	100	547.334	-	3,6,9,12,15,18,21,24,27,30,33-Undecaoxapentatriacontane-1,35-diol	Alcohol	suspected
5.801	3.451	$C_{27}H_{51}N_4O_{10}$	39.54	591.3591	-	Unknown	-	-
6.048	3.564	$C_{29}H_{55}N_4O_{11}$	79.13	635.3876	-	Unknown	-	-
6.245	2.684	$C_{31}H_{59}N_4O_{12}$	90.07	679.413	-	Unknown	-	-
6.442	2.116	$C_{32}H_{67}O_{17}$	72.52	723.4389	-	Unknown	-	-
6.596	1.609	$C_{34}H_{71}O_{18}$	94.37	767.4642	-	Unknown	-	-

6.751	1.222	$C_{36}H_{75}O_{19}$	95.71	811.4905	-	Unknown	-	-
6.885	1.03	$C_{38}H_{82}NO_{20}$	94.53	872.5433	-	Unknown	-	-
6.99	1.22	$C_{40}H_{86}NO_{21}$	90.31	916.5695	-	Unknown	-	-
7.103	1.453	$C_{42}H_{90}NO_{22}$	95.15	960.5958	-	Unknown	-	-
7.32	1.16	$C_{38}H_{82}N_{25}O_8S$	85.8	1048.6501	-	Unknown	-	-
7.672	0.097	$C_{18}H_{30}NO_2$	83.68	292.2281	-	1-(2-Cyclopentylphenoxy)-3-[(2-methyl-2-propanyl)amino]-2-propanol	Alcohol	suspected
7.827	0.379	$C_{29}H_{42}NO_3$	46.92	452.3129	-	Unknown	-	-
7.961	0.1	$C_{29}H_{42}NO_3$	47.34	452.3134	-	Unknown	-	-
8.178	0.308	$C_{25}H_{38}N_7O$	51.73	452.3128	-	Unknown	-	-
8.354	0.279	$C_{27}H_{39}O$	77.05	379.2964	-	22E)-Cholesta-4,6,8(14),22-tetraen-3-one	Steroid	suspected
8.593	0.167	$C_{28}H_{41}O$	33.01	393.3117	-	Unknown	-	-
8.789	0.984	$C_{15}H_{30}N$	n/a	224.2389	-	Unknown	-	-
8.994	0.399	$C_{24}H_{41}N_2O_5$	55.35	437.302	-	Unknown	-	-
9.296	0.595	$C_{20}H_{33}O_5$	91.59	353.2308	-	(11α,13E,15S)-11,15-Dihydroxy-9-oxoprost-13-en-1-oate	Eicosanoid	suspected
9.43	0.061	$C_{25}H_{35}OS_2$	95.34	415.2126	-	Unknown	-	-
9.647	0.055	$C_{20}H_{21}O_8$	73.61	389.1239	-	Unknown	-	-
9.915	0.377	$C_{22}H_{33}O_5$	88.4	377.2311	-	Resolvin D2	Eicosanoid	suspected
10.267	0.842	$C_{22}H_{40}N_3O_2$	64.68	378.3126	-	Unknown	-	-
10.547	0.256	$C_{17}H_{34}NO$	97.72	268.2652	-	1-Isocyanatohexadecane	Isocyanate	suspected
11.011	4.764	$C_{18}H_{36}NO$	99.39	282.2813	55.0547; 69.0707; 83.0865	Dodemorph	Morpholine	confirmed
11.3	0.855	$C_{18}H_{38}NO$	n/a	284.2963	-	Unknown	-	-
11.426	0.621	$C_{24}H_{44}N_3O_2$	45.12	406.3435	-	Unknown	-	-
11.673	0.397	$C_{29}H_{47}N_2O$	53.48	439.3647	-	Unknown	-	-
11.848	0.725	$C_{25}H_{46}NO_4$	66.53	424.3429	-	Unknown	-	-
12.179	3.99	$C_{24}H_{42}N_5$	65.34	400.3436	-	Unknown	-	-
12.418	4.47	$C_{26}H_{44}N_5$	86.08	426.3602	-	N-[6-(1-Piperidinyl)hexyl]-1-[3-(1-piperidinyl)propyl]-1H-indazol-3-amine	Indazole	suspected
13.1	13.3	$C_{26}H_{46}N_5$	82.3	428.3742	-	Unknown	-	-
13.564	11.94	$C_{26}H_{46}N_3O_6$	79.34	496.3406	-	(2R,4S,5S,7S)-5-Amino-N-(3-amino-3-oxopropyl)-4-hydroxy-7-[4-methoxy-3-(3-methoxypropoxy)benzyl]-2,8-dimethylnonanamide	Amide	suspected
13.958	5.238	$C_{28}H_{48}N_3O_6$	60.94	522.3568	-	Unknown	-	-
14.443	1.708	$C_{46}H_{96}NO_{17}$	81.08	934.6672	-	Unknown	-	-
14.682	0.415	$C_{40}H_{84}N_{25}O_2S$	99.62	978.6937	-	Unknown	-	-
15.385	2.234	$C_{28}H_{50}N_3O_6$	60.88	524.3726	-	Unknown	-	-
15.602	0.405	$C_{20}H_{40}NO_2$	96.64	326.3063	69.0704; 149.0455; 207.0333; 267.0002; 309.2793	Oleoyl Ethanolamide	Ester	confirmed
15.778	0.609	$C_{16}H_{34}NO$	n/a	256.2648	-	Unknown	-	-
16.046	0.18	$C_{18}H_{36}NO$	100	282.2802	57,0694; 69,0694; 69,0697; 81,0694; 83,0855; 85,1008; 97,1016; 111,1182; 111,1165	4-Cyclododecyl-2,6-dimethylmorpholine	Morpholine	confirmed
16.222	0.566	$C_{38}H_{49}O_6$	41.6	601.3511	-	Unknown	-	-
16.439	0.116	$C_{23}H_{45}N_2O_2S$	45.64	413.3243	-	Unknown	-	-
16.657	0.883	$C_{20}H_{42}NO_2$	99.99	328.3223	-	N-(2-Hydroxyethyl) octadecanamide	N-acylethanolamines	suspected
16.812	0.255	$C_{42}H_{79}O_{14}$	38.57	807.5455	-	Unknown	-	-

17.142	0.039	$C_{18}H_{38}NO$	n/a	284.2953	-	Unknown	-	-
17.557	0.093	$C_{33}H_{61}N_2O_6S$	38.77	613.4296	-	Unknown	-	-
17.691	0.215	$C_{32}H_{57}O_8$	88.03	569.4036	-	(3*β*,5*α*,6*α*,15*β*,24S)-3,6,15-Trihydroxycholestan-24-yl *β*-D-xylopyranoside	Glycoside	suspected
17.824	0.454	$C_{10}H_{42}N_{27}O$	41.77	556.4067	-	Unknown	-	-
17.979	2.848	$C_{44}H_{87}N_6O_{14}$	82.86	923.6282	-	Unknown	-	-
18.414	0.747	$C_{27}H_{43}$	99.57	367.3372	-	Cholesta-2,4,6-triene	Steroid	suspected
18.879	3.193	$C_{27}H_{45}O_2$	99.19	401.3419	-	(5E,7E)-9,10-Secocholesta-5,7,10-triene-3,25-diol	Steroid	suspected

Table 3 Drug-likeliness of ligand candidates.

Compound	Formula	MW (g/mol)	Hydrogen bond donor	Hydrogen bond acceptor	Log P	Lipinski*	Predicted Toxicity Class**
Carnitine	$C_7H_{15}NO_3$	161.10	1	3	-2.4	0	VI
Hypoxanthine	$C_5H_4N_4O$	136.03	2	3	-0.35	0	IV
Indoline	C_8H_9N	119.07	1	1	1.65	0	IV
Resolvin D2	$C_{22}H_{32}O_5$	376.22	4	4	2.47	0	V
(11*α*,13E,15S)-11,15-Dihydroxy-9-oxoprost-13-en-1-oate	$C_{20}H_{33}O_5$	353.23	2	5	1.98	0	III
1-Dodecanol	$C_{12}H_{26}O$	186.19	1	1	3.41	0	IV
Pentanedioic acid, 2,4-dimethyl-, dimethyl ester	$C_9H_{16}O_4$	188.10	0	4	1.25	0	V

*Number on Lipinski column means the amount of Lipinki's rule violated. Zero means no Lipinski's rule violated;
** Class III: toxic if swallowed ($50 < LD50 \leq 300$), Class IV: harmful if swallowed ($300 < LD_{50} \leq 2000$), Class V: may be harmful if swallowed ($2000 < LD50 \leq 5000$), Class VI: non-toxic ($LD50 > 5000$).

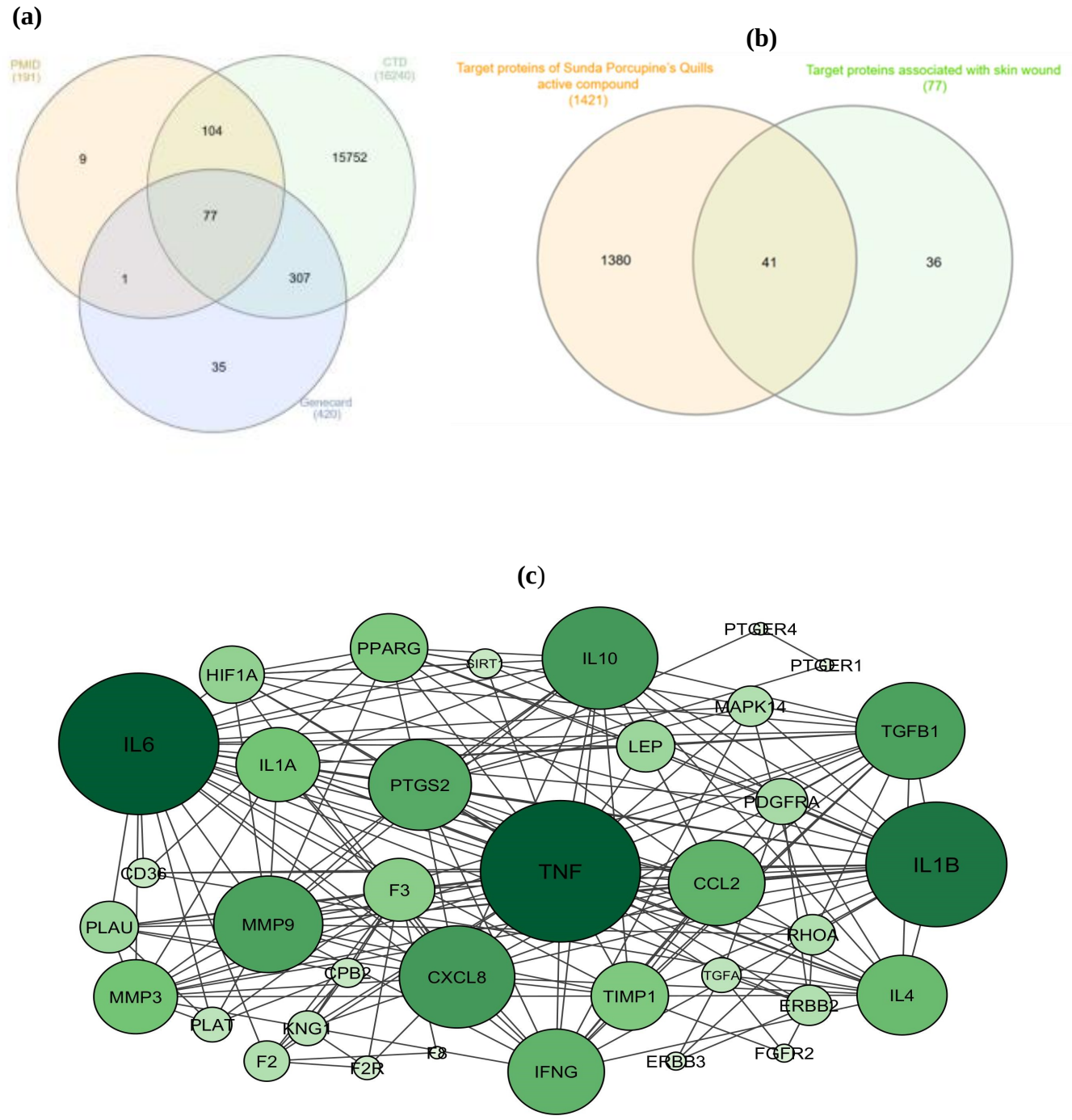

Fig. 3 Target of network pharmacology: (a) Intersection Venn diagram of target proteins associated with skin wound healing , (b) Intersection Venn diagram potential target between target proteins associated with skin wound and target proteins of Sunda porcupine's quills active compound , (c) PPI network of potential target selected with ≥3 degree level. Different colors and sizes represent the degree of freedom. The darker colors indicate a greater degree of freedom.

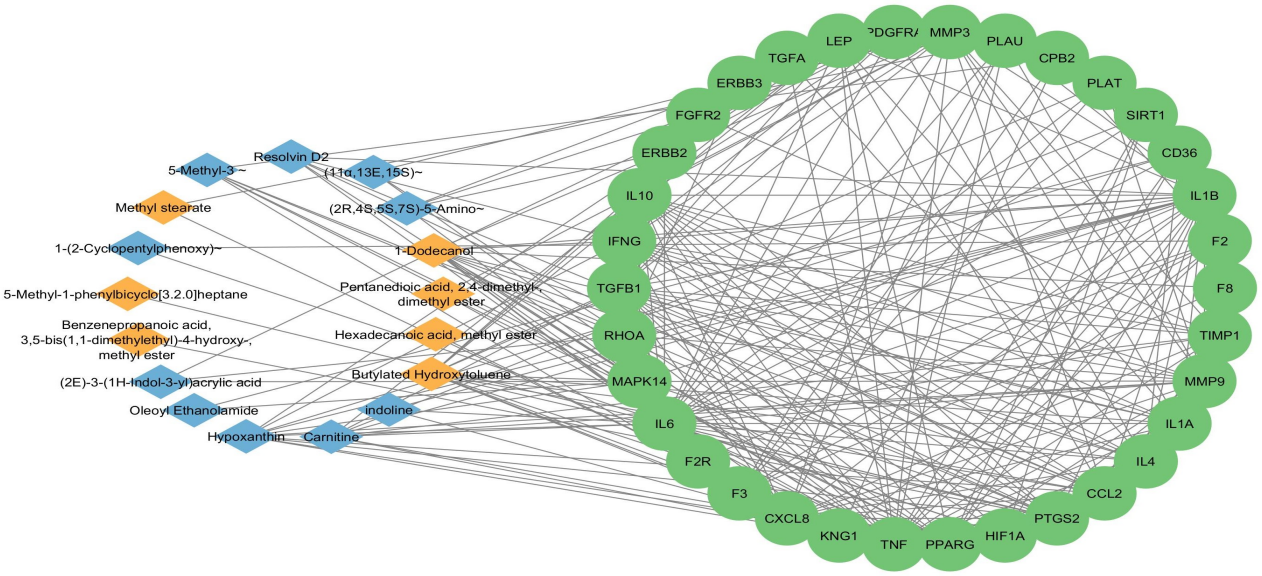

Fig. 4 Compound-target network of Sunda porcupine's quills extract compounds related to skin wound healing . The blue dots represent *Hystrix javanica* compound of UPLC-MS/MS, orange dots represent Sunda porcupine's quills extract compounds of GC-MS,and the green dots represent protein targets.

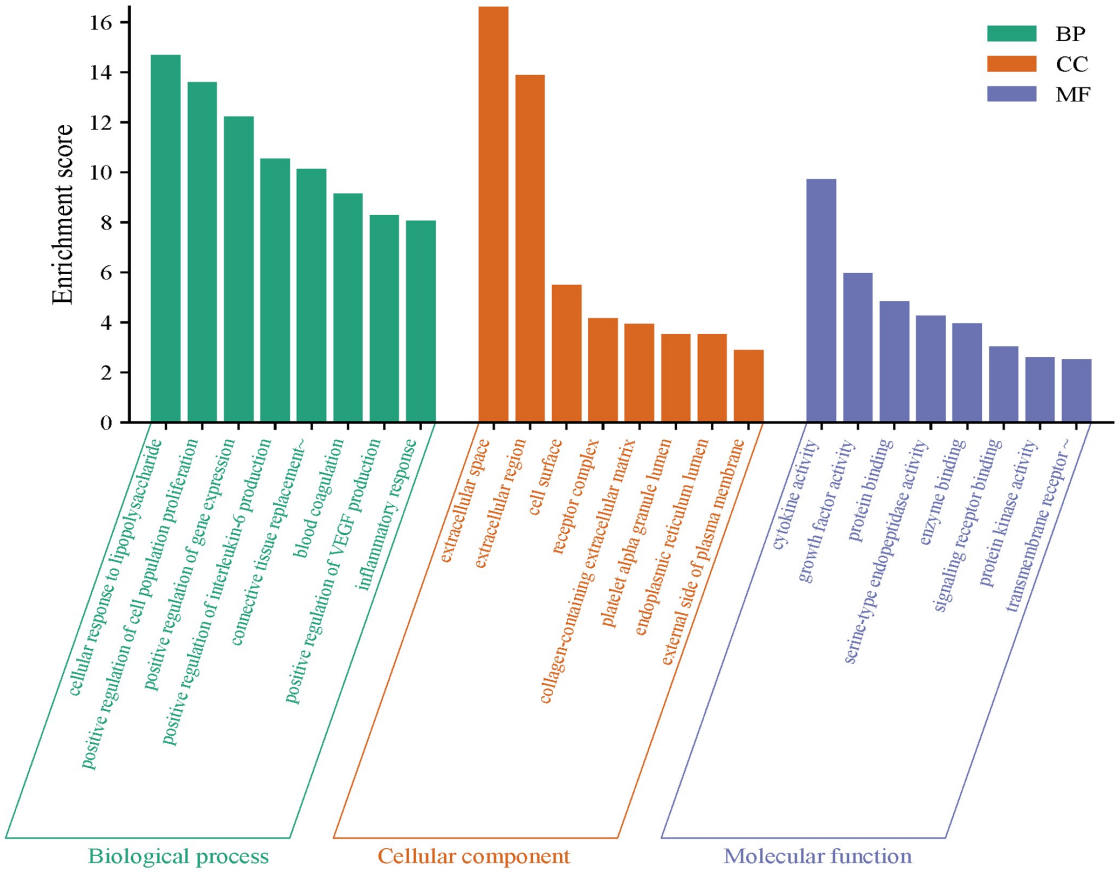

Fig. 5 Gene ontology enrichment.

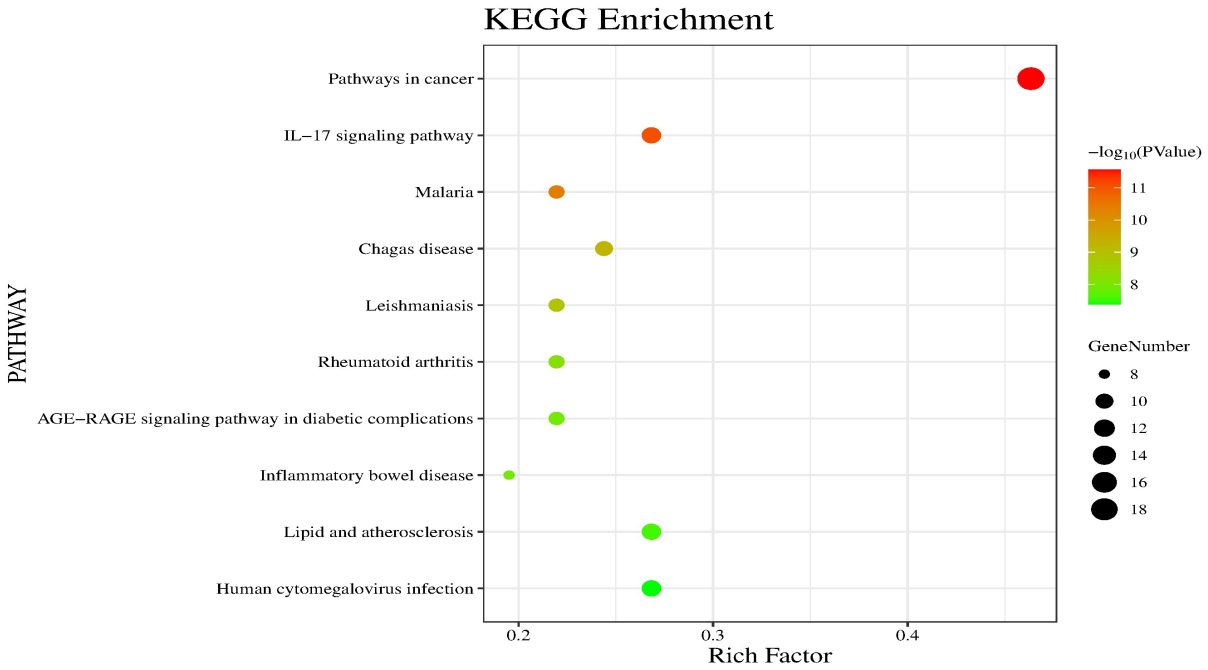

Fig. 6 KEGG enrichment showing the top 10 enriched pathways.

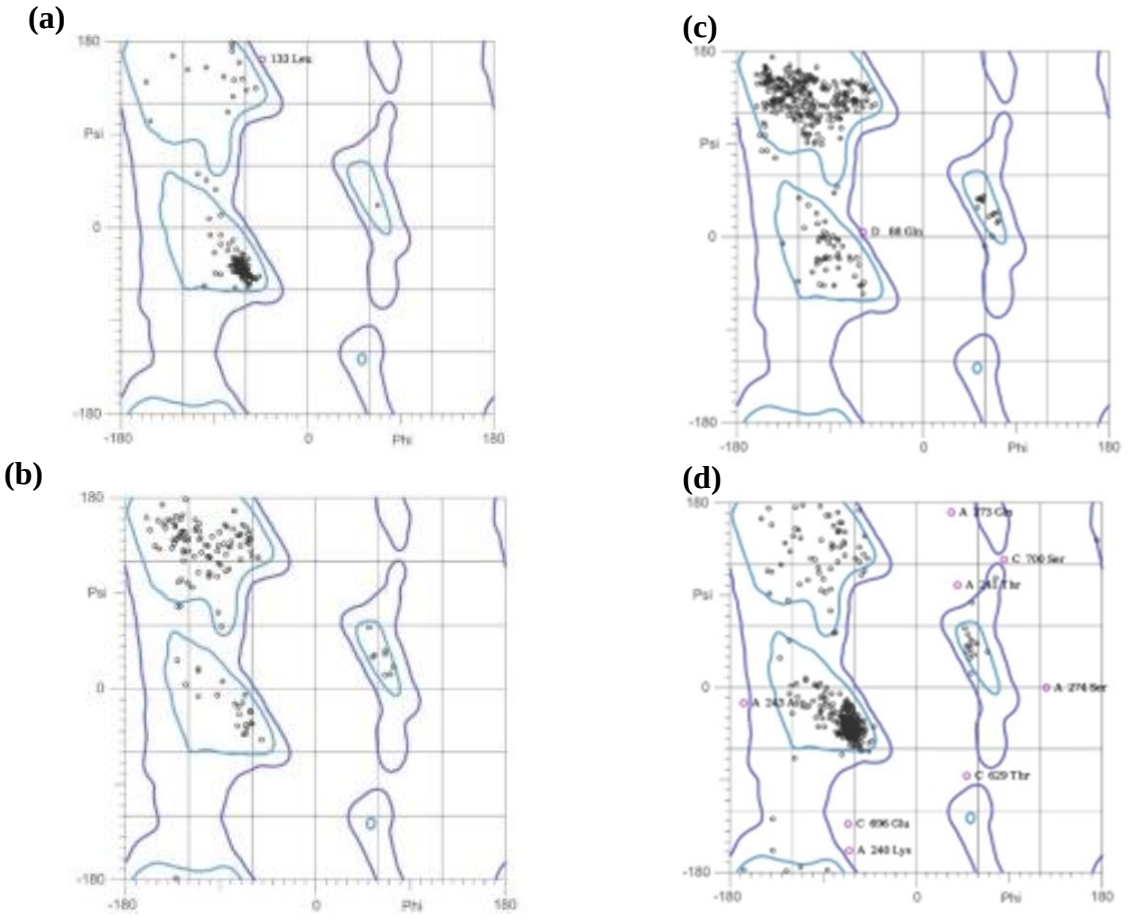

Fig. 7 Ramachandran Plot of (a) IL6, (b) IL1β, (c) TNFα, and (d) PPARγ.

Table 4 Interaction between top 7 identified compounds from Sunda porcupine's quills extract (ligand) with selected wound healing receptors.

No	Protein (PDB)	Reference ligand [interacted amino acid residues]	Binding energy (kcal/mol)	Test ligand	Binding energy (kcal/mol)	Amino acid residues interacted with test ligand
1	IL6 (1ALU)	L(+)-Tartaric Acid [GLU A:23, ARG A:24]	-3.58	(11α,13E,15S)-11,15-Dihydroxy-9-oxoprost-13-en-1-oate	-5.04	ARG A:182, ARG A:179, ARG A:30
				Pentanedioic acid, 2,4-dimethyl-, dimethyl ester	-4.46	LEU A:178, ARG A:179, ARG A:182, ARG A:30
				ResolvinD2	-4.13	LEU A:33, ARG A:179, ARG A:182, LEU A: 178, ARG A:30
				Hypoxanthine	-3.64	GLN A: 175
				Carnitine	-4.16	ARG A:182, ARG A:179, GLN A: 175
				1-Dodecanol	-3.30	ASP A:26, LEU A:178, ARG A:30, ARG A:179
				Indoline	-3.08	LEU A:178, GLN A: 175, ARG A: 182
2	IL1β (5R86)	GT4 [MET A:148, LYS A:103, LEU A:110]	-5.78	ResolvinD2	-6.71	ILE A:56, LEU A:110, PHE A:150, MET A:148
				Pentanedioic acid, 2,4-dimethyl-, dimethyl ester	-5.13	MET A:148, LYS A:103, PHE A:150, THR A:147
				Hypoxanthine	-4.75	ASN A:108, MET A:148
				Carnitine	-4.03	LYS A:103
				1-Dodecanol	-4.08	MET A:148, LEU A:110, GLU A:105, PHE A:150
				(11α,13E,15S)-11,15-Dihydroxy-9-oxoprost-13-en-1-oate	-6.41	PHE A:150, PHE A:46, MET A:148, LEU A:110, ASN A:108
				Indoline	-4.68	LEU A:110, MET A: 148
3	TNFα (2AZ5)	Ligand ID: 307 [TYR D:119, TYR D:59, TYR D:151, GLY C:121, TYR C:149]	-9.59	ResolvinD2	-5.27	TYR C:59
				Hypoxanthine	-4.06	LEU D:120, SER D:60, GLY C:121
				Carnitine	-3.13	TYR D:59, GLY C:121, TYR D:151
				Indoline	-4.50	SER D:60, LEU D:120, TYR D:119
				Pentanedioic acid, 2,4-dimethyl-, dimethyl ester	-4.70	TYR D:59, TYR D:119, TYR C:151, TYR C:119, SESR C:60, LEU C:120, TYR D:151, SER D:60
				(11α,13E,15S)-11,15-Dihydroxy-9-oxoprost-13-en-1-oate	-6.53	TYR C:119, TYR C:151, LEU D:120, TYR C:59
				1-Dodecanol	-4.53	SER C:60, LEU C:120, TYR D:119

4	PPARγ (2PRG)	Thiazolidinedione [TYR A:473, HIS A:323, SER A:289, GLN A:286, HIS A:449, ILE A:326, LEU A:330, CYS A:285, TYR A:327, MET A:364, LEU A:353, VAL A:339, MET A:348, LEU 340]	-9.78	ResolvinD2	-8.14	SER A:342, LEU A:333, ARG A:288, LEU A:330, TYR A:473, ILE A:326, ALA A:292, TYR A:327, HIS A:449, PHE A:363
				Hypoxanthine	-4.60	GLN A:286, TYR A:473
				Indoline	-4.56	HIS A:449, TYR A:327, CYS A:285
				Pentanedioic acid, 2,4-methyl-, dimethyl ester	-5.6	TYR A:327, HIS A:323, ILE A:326, HIS A:449, CYS A:285, TYR A:473, LEU A:469
				Carnitine	-4.81	SER A:289, HIS A:323, TYR A473, GLN A286, HIS A449
				1-Dodecanol	-5.27	ARG A:288, CYS A:285, LEU A:330, ILE A:326, MET A:364, HIS A:449, TYR A:327, TYR A:473
				(11α,13E,15S)-11,15-Dihydroxy-9-oxoprost-13-en-1-oate	-7.79	CYS A:A85, LEU A:330, ARG A:288, SER A:342, PHE A:287, LEU A:270

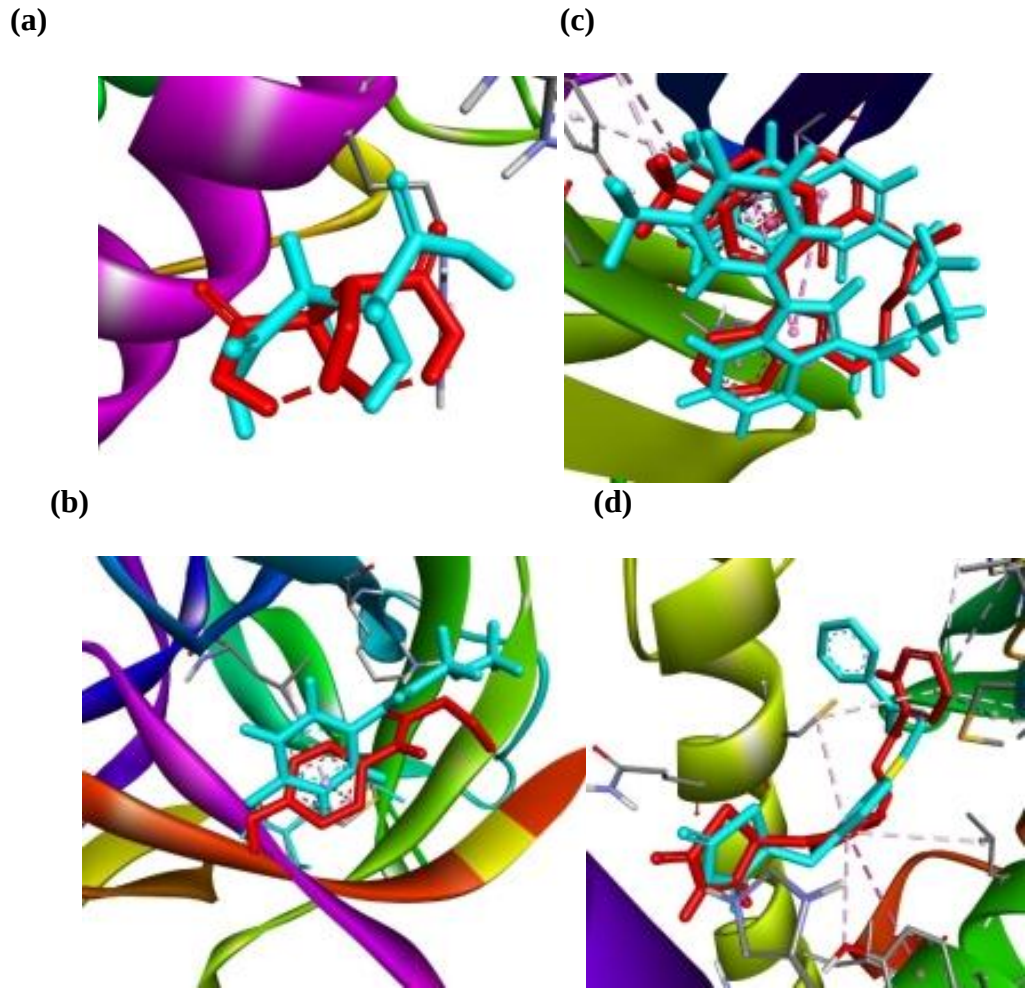

Fig. 8 Molecular docking validation (a) Superimposition of L(+)-tartaric Acid in initial (turquoise) and redocking (red) positions on IL6 (PDB ID: 1ALU) with RMSD 0.887 Å; (b) Superimposition of GT4 in initial (turquoise) and redocking (red) positions on IL1β (PDB ID: 5R86) with RMSD 1.018 Å; (c) Superimposition of 307 ligand in initial (turquoise) and redocking (red) positions on TNFα (PDB ID: 2AZ5) with RMSD 1.022 Å; (d) Superimposition of Thiazolidinedione in initial (turquoise) and redocking (red) positions on PPARγ (PDB ID: 2PRG) with RMSD 1.648 Å.

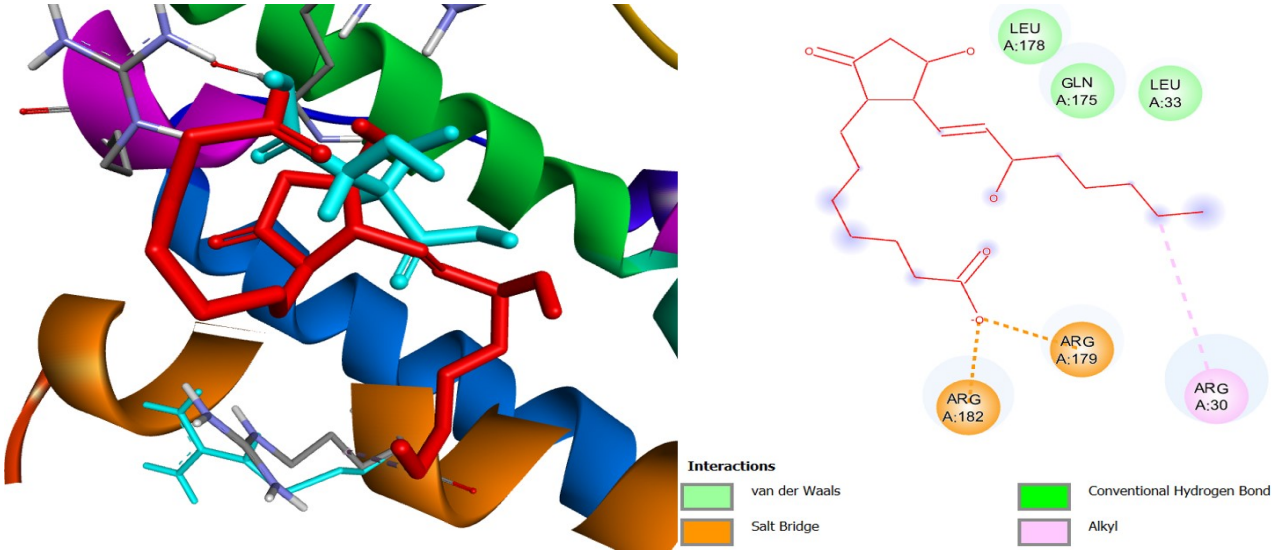

Fig. 9 Visualization of the interaction of the (11α,13E,15S)-11,15-dihydroxy-9-oxoprost-13-en-1-oate (red) with IL6 protein.

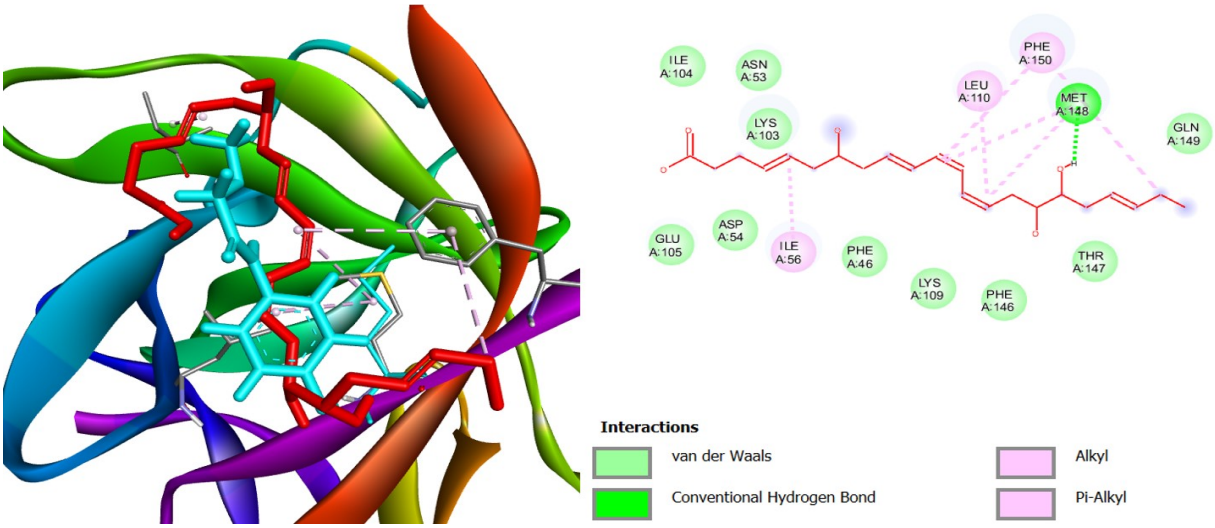

Fig. 10 Visualization of the interaction of the test ligands resolvinD2 (red) with IL1β protein.

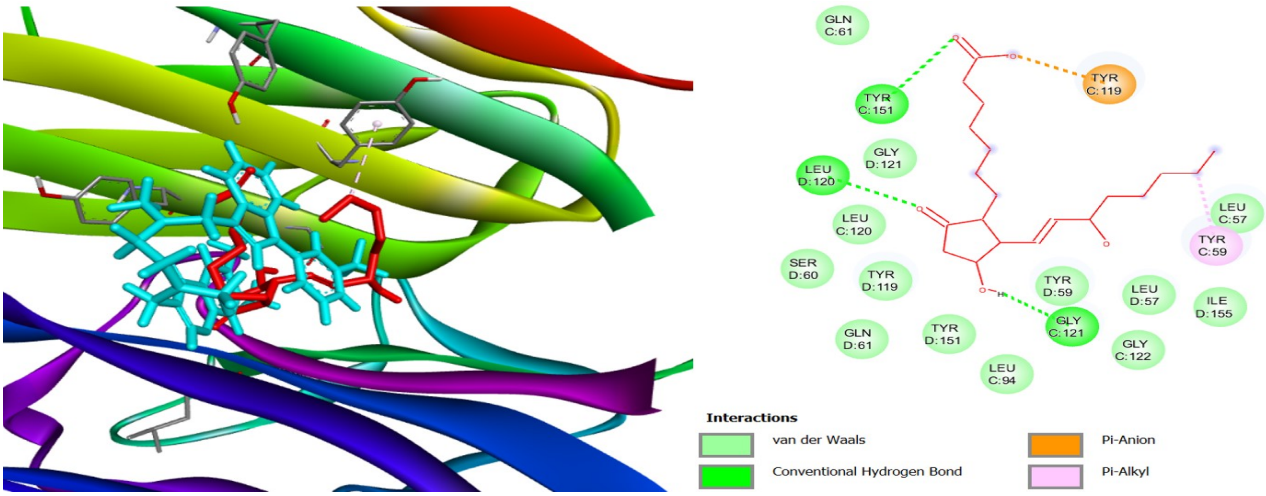

Fig. 11 Visualization of the interaction of the (11α,13E,15S)-11,15-dihydroxy-9-oxoprost-13-en-1-oate (red) with TNFα protein.

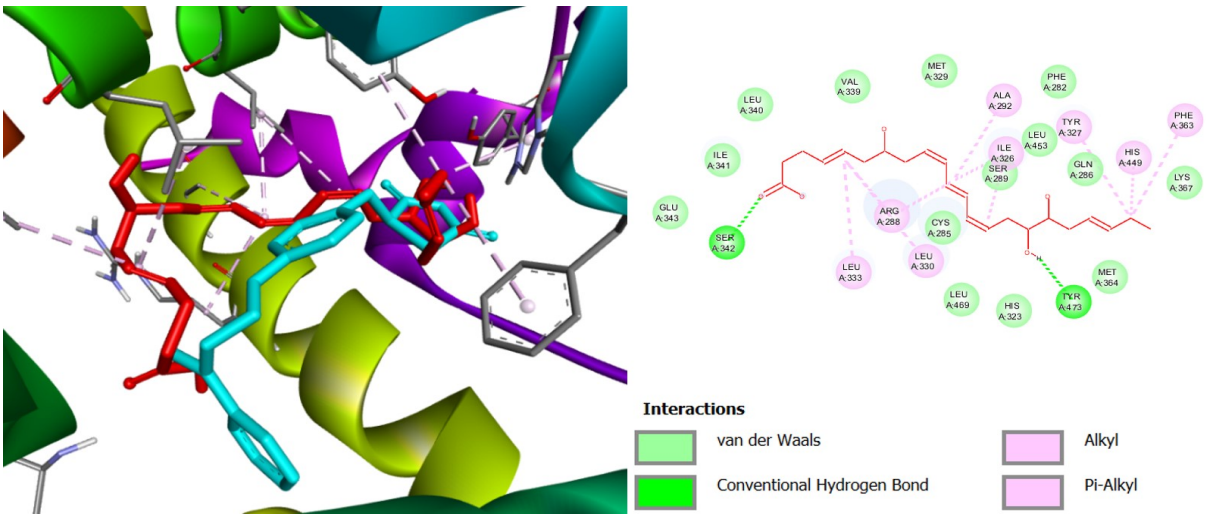

Fig. 12 Visualization of the interaction of the resolvinD2 (red) with PPARγ protein.

Discussion

Our study identified 32 compounds from the ethanolic crude extract obtained from Sunda porcupine's quills based on GC-MS and UPLC-MS/MS. These compounds included well-known purines, indoles, amino acid derivatives, pyrazoles, alkaloids, alcohols, steroids, eicosanoids, isocyanates, morpholines, indazoles, amides, esters, morpholines, N-acylethanolamines, glycosides, and carboxylic acids. The wound healing process typically involves phases of haemostasis, inflammation, proliferation, and remodeling [13]. It is crucial to understand the mode of action of compounds during the phases of wound healing. We investigated how Sunda porcupine's quills can help reduce skin wounds by analyzing a network pharmacology between Sunda porcupine's quill components and target proteins associated with wound healing. We identified several critical proteins in the PPI network such as RHOA, HSPβ1, HIF1α, CXCL8, IL6, TNFα, IL1β, IL10, IFNγ, PTGS2, MMP9, MMP3, LEP, IGF1, PPARγ, CD36, MAPK14, PLAU, CDKN1A, INS, F2, TGF-β1, TIMP1, SIRT1, and CCL2. In addition, our research showed that nodes IL6, TNFα, and IL1β exhibited a high degree of connectivity and centrality. The identification of molecules that play an essential role in the binding between a ligand and a receptor required the analysis of connectivity and centrality parameters. These molecules are often referred to as potential targets and are distinguished by their high levels of connectivity and centrality within the molecular interaction network. Connectivity is the number of interactions a molecule has with other molecules present in the binding site, with molecules exhibiting high connectivity being more likely to be involved in the binding process. Centrality measures of the importance of a molecule within the binding site, with molecules exhibiting high centrality frequently located at the center of the binding site and critical to the binding process.

IL6 is a proinflammatory cytokine that regulates TGF-β1 expression in the skin and fibroblasts. TGF-β1 influences inflammation, angiogenesis, collagen production, and wound contraction by stimulating various cell types [14]. A previous study found that upregulated IL-6 levels in rats lead to increased inflammation and skin growth [15]. TNFα is a cytokine that regulates inflammation and promotes the proliferation and apoptosis of cells. It also stimulates the production of other cytokines, such as IL6 and IL10, and can induce the expression of PTGS2 [16]. Studies have demonstrated that TNFα can impair the wound healing process, suggesting that inhibiting it may represent a potential therapeutic approach to enhance the healing of abnormal wounds [16-17]. IL1β is another proinflammatory cytokine that, together with TNFα and IL6, recruits immune cells to the wound site [18]. The study was conducted by Russo et al. and Soliman et al. who found that IL1β increases human keratinocyte growth factor gene expression in fibroblasts, promoting re-epithelialization of the skin [19-20]. The top pathways related to Sunda porcupine's quills extract in the biological process of GO enrichment include a positive cellular response to lipopolysaccharide. Interestingly, our KEGG analysis revealed that the pathways with the highest score were pathways in cancer. However, relevant pathways for skin wound healing may include the IL-17 signaling pathway, which involves inflammation [17,21]. Inflammation is the first phase of wound healing, playing a critical role in combating pathogens by recruiting cells to the wound site, removing wound debris, and triggering keratinocyte proliferation. Like a double-edged sword, excessive inflammation in the wound can also impair and delay healing [20]. By combining the results of PPI with KEGG, we speculate that IL6, TNFα, and IL1β nodes may represent potential targets for inhibiting the excessive acute inflammation phase.

The Sunda porcupine's quills extract and skin wound healing receptors network diagram revealed that the main nodes involved in wound healing are carnitine, indoline, resolvin-D2, hypoxanthine, and (11α,13E,15S)-11,15-dihydroxy-9-oxoprost-13-en-1-oate. A previous study has reported that L-carnitine supplements can significantly reduce IL6 levels, thereby reducing

inflammation [22]. Carnitine can also increase PPARγ protein expression in insulin resistance [23]. In vivo studies have demonstrated that L-carnitine treatment reduces oxidative stress, preventing the expression of TNFα, IL6, and NF-κB in rats [24]. Pre-treatment with L-carnitine has also been shown to induce a significcant reduction in MMP-9 expression [25]. Indoline is an aromatic substance with the chemical formula C_8H_9N. It has been used as an anaesthetic, and some studies have indicated that indoline derivatives can suppress inflammation in lipopolysaccharide (LPS)-activated macrophages, reducing TNFα and IL-6 [26]. Other studies have reported that indoline derivatives have protective effects by down-regulating IL1β, IL6, and TNFα in neuroinflammation [27].

Resolvin-D2 (RvD2) is a metabolite derived from omega-3 fatty acids. Some studies have shown that RvD2 can reduce IL-6 levels in human umbilical artery smooth muscle cells (HUASMC) stimulated with LPS [28]. In mice peritonitis models, RvD2 decreased IL1β, IL-6, and TNFα levels in LPS-treated mice [29]. Additionally, when bone marrow-derived macrophage (BMDM) cells were stimulated with LPS, RvD2 significantly reduced PTGS2 mRNA expression in vitro [30]. RvD2 has also been found to reduce the expression of genes PTGS2, which is involved in the production of prostaglandins [31]. Hypoxanthine is a purine base that is involved in DNA synthesis and repair. A few studies suggest that MMP9 in brain edema after ischemic stroke may be associated with elevated plasma hypoxanthine levels [32]. (11α,13E,15S)-11,15-Dihydroxy-9-oxoprost-13-en-1-oate, particularly alprostadil interacts with TNFα, IL6 and IL1β by inhibiting their production in acute respiratory distress syndrome and LPS induced cardiomyocyte injury [33–35]. Alprostadil also has been shown to reduce the incidence of partial wound necrosis in ischemic wounds and shorten the average recovery time [36]. The components present in Sunda porcupine's quills extract may indirectly influence the target protein by modulating its expression or regulating its activity. The Sunda porcupine's quills extract speculated wound healing potential could be attributed to achieve its effects through the synergistic effect of multiple compounds interacting with specific proteins to regulate inflammation.

Molecular docking studies have revealed that specific compounds have the potential to bind to IL6, IL1β, and TNFα, which exhibit top degrees of centrality, characterized by different binding free energies (ΔG). Lower or more negative ΔG values indicate greater binding affinity between the ligand and protein, resulting in more stable binding [37]. Receptor of IL6, IL1β, and TNFα were selected as primary targets due to their high degree values in the PPI network and their consistent presence in both PPI and KEGG pathways, highlighting their important role in the acute inflammatory phase. We also used PPARγ as a representative candidate for target inhibition of the proliferation phase because its activation causes the inhibition of epidermal keratinocyte proliferation [38-39]. The screening of compounds as candidate ligands for molecular docking was conducted based on predicted drug characteristics, including adherence to Lipinski's rule of five and toxicity classification. According to Lipinski's rule of five, seven test ligands were found to possess potential drug-likeliness properties. The toxicity analysis categorized these ligands within classes III to VI. In line with our previous study, the toxicity evaluation of the Sunda porcupine's quills extract indicated that it is non-toxic, as classified by the Globally Harmonized System (GHS) [40].

Resolvin-D2, hypoxanthine, carnitine, indoline, pentanedioic acid 2,4-dimethyl-dimethyl ester, (11α,13E,15S)-11,15-dihydroxy-9-oxoprost-13-en-1-oate, and 1-dodecanol demonstrated as ligands binding to IL6, IL1β, TNFα, and PPARγ with negative ΔG values. Among these, resolvin-D2, pentanedioic acid 2,4-dimethyl-dimethyl ester, (11α,13E,15S)-11,15-dihydroxy-9-oxoprost-13-en-1-oate, and carnitine exhibited more negative binding energies than that of the natural native ligand of IL6, L(+)-tartaric acid, suggesting that these three compounds may strongly inhibit the IL6 pathway in skin wound healing . On the other hand, hypoxanthine has binding energies equivalent to the natural native ligand of IL6, suggesting that it may intermediately inhibit the IL6 pathway. Additionally, resolvin-D2 and (11α,13E,15S)-11,15-dihydroxy-9-oxoprost-13-en-1-oat achieved the highest ΔG values compared with natural native ligand of IL1β (GT4), indicating that these compounds may strongly inhibit IL1β. However, none of the ligands, namely resolvin-D2, hypoxanthine, carnitine, indoline, pentanedioic acid 2,4-dimethyl-dimethyl ester, (11α,13E,15S)-11,15-dihydroxy-9-oxoprost-13-en-1-oate, and 1-dodecanol had a more negative □G value compared to those of the natural native ligand of TNFα (6,7-dimethyl-3-[(methyl{2-[methyl({1-[3-(trifluoromethyl) phenyl]-1h-indol-3-yl} methyl) amino] ethyl} amino) methyl]-4h-chromen-4-one (ID: 307)) and the natural native ligand of PPARγ (thiazolidinedione), thus these compounds have less potential to inhibit TNFα and PPARγ pathways. Further experiments, including in vitro and in vivo studies, are required to validate the potential of Sunda porcupine's quills extract in skin wound healing.

Conclusion

The untargeted metabolomic study of Sunda porcupine's quills extract was successfully conducted using GC-MS and UPLC-MS/MS, identifying 32 compounds. By integrating network pharmacology and molecular docking, the study revealed that resolvin-D2, hypoxanthine, carnitine, indoline, pentanedioic acid 2,4-dimethyl-dimethyl ester, (11α,13E,15S)-11,15-dihydroxy-9-oxoprost-13-en-1-oate, and 1-dodecanol have the potential to inhibit the binding of proinflammatory cytokines such as IL6, IL1β, TNFα, and PPARγ as indicated by their negative □G scores. Interestingly, resolvin-D2, pentanedioic acid 2,4-dimethyl-dimethyl ester, (11α,13E,15S)-11,15-dihydroxy-9-oxoprost-13-en-1-oate, and carnitine demonstrated stronger inhibition of IL6, while resolvin-D2 and (11α,13E,15S)-11,15-dihydroxy-9-oxoprost-13-en-1-oate achieved more negative □G score compared to

reference ligands, indicating stronger potential as IL1β inhibitors. However, all test ligands showed a weak potential as TNFα and PPARγ inhibitors. These findings suggest a promising therapeutic potential of Sunda porcupine's quills extract for traditional wound healing treatments. Further research is required to determine chemical structure and biological relevance of unidentified peaks and unknown compounds on Sunda porcupine's quills extract. Moreover, in vivo and in vitro studies are necessary to validate the potential of Sunda porcupine's quills as skin wound healing agent.

Conflicts of interest

The authors declare that there are no conflicts of interest.

Acknowledgment

We thank the Central Board of Muhammadiyah, Indonesia for funding the research through the Muhammadiyah National Research Grant. We also thank the National Research and Innovation Agency of Indonesia for facilitating the research.

Funding

This research was funded by the Muhammadiyah National Research Grant Batch VII Year 2024 as per Research Contract Letter No. 0258.233/1.3/D/2024.

Authors' contributions

Budiman MA contributed to the concept, design, data acquisition, data analysis, manuscript preparation, and served as a guarantor. Sari SDP conducted the literature search, data acquisition, and manuscript preparation and editing. Elfirta RR involved in the design, intellectual content, literature search, data analysis, and manuscript review. Masrukhin contributed to the literature search, data acquisition, data analysis, and manuscript editing. Nugroho HA worked in the intellectual content, data analysis, manuscript preparation, and manuscript review. Amalia RLR assisted with data acquisition manuscript preparation, and manuscript editing. Farida WR contributed to the concept, intellectual content, manuscript editing and review, and acted as a guarantor. Ferdian PR was responsible for the concept, design, intellectual content, data analysis, manuscript review, and also served as a guarantor.

Ethical considerations

The collection of Sunda porcupine's quills was conducted in 2019 as part of a physiological study. Ethical clearance of the research was approved by the Indonesian Institute of Sciences with protocol number B-15897/IPH/KS/02/04/XII/2019.

References

1. Lu Y, Wang Y, Wang J, Liang L, Li J, Yu Y, et al. A Comprehensive Exploration of Hydrogel Application in Multistage Skin Wound Healing. Biomater Sci 2024; 12(15): 3745-3764. doi: 10.1039/d4bm00394b.
2. Trinh XT, Long N Van, Van Anh LT, Nga PT, Giang NN, Chien PN, et al. A comprehensive review of natural compounds for wound healing: targeting bioactivity perspective. International Journal of Molecular Sciences 2022; 23 (17). doi: 10.3390/ijms23179573.
3. Joyce K, Fabra GT, Bozkurt Y, Pandit A. Bioactive potential of natural biomaterials : identification, retention and assessment of biological properties. Signal Transduct Target Ther 2021; 6(122): 1-28. doi: 10.1038/s41392-021-00512-8.
4. Prawira AY, Hosaka YZ, Novelina S, Farida WR, Darusman HS, Agungpriyono S. Morphological evaluation of polysaccharide content and collagen composition during cutaneous wound healing in the sunda porcupine (*Hystrix javanica*). J Vet Med Sci 2020; 82(5): 506-515. doi: 10.1292/jvms.19-0603.
5. Agungpriyono S, Pristihadi D, Sutardi L, Prawira AY, Farida WR, Dewi T. Comparison of burn and incision wound healing in rat given crude extract of porcupine quill (*Hystrix* sp.). Front Sustain Agromaritime Environ Dev Conf 2024; 1359: 1-8. doi: 10.1088/1755-1315/1359/1/012137.
6. Inayah N. Potensi pengembangan landak (Hystrix sp.) sebagai Produk komersial. Fauna Indones 2016;15(2):37–43.
7. Krisyanto RD, Ardian H, Anwari MS. Kajian etnozoologi untuk pengobatan suku Dayaksebaruk di Desa Setunggul Kecamatan Silat Hilir Kabupaten Kapuas Hulu. J Hutan Lestari 2019;7(3):1282–9. doi: https://doi.org/10.26418/jhl.v7i3.37405.
8. Budiman MA, Ferdian PR, Handayani TH, Elfirta RR, Masrukhin, Nugroho HA, et al. Investigation of antioxidant and antimicrobial properties of sunda porcupine's (*Hystrix javanica*, F.Cuvier 1823) quills ethanolic crude extract. Trop Life Sci Res 2024; 35(3): 1–21. doi: 10.21315/tlsr2024.35.3.1.
9. Zuhri UM, Purwaningsih EH, Fadilah F, Yuliana ND. Network pharmacology integrated molecular dynamics reveals the bioactive compounds and potential targets of Tinospora crispa Linn. as insulin sensitizer. PLoS One 2022; 17(6): 1-15. doi. 10.1371/journal.pone.0251837.
10. Mo L, Wang Z, Huang H, Li J, Ma C, Zhang J, et al. Integrated analysis of crucial genes and miRNAs associated with osteoporotic fracture of type 2 diabetes. Biomed Res Int 2022. doi: 10.1155/2022/3921570.
11. Guan M, Guo L, Ma H, Wu H, Fan X. Network pharmacology and molecular docking suggest the mechanism for biological activity of rosmarinic acid. Evidence-based Complement Altern Med 2021. doi: 10.1155/2021/5190808.
12. Zhou G, Feng X, Tao A. Explore the lipid-lowering and weight-reducing mechanism of lotus leaf based on network pharmacology and molecular docking. Evidence-based Complement Altern Med. 2021. doi: 10.1155/2021/1464027.
13. Yang F, Bai X, Dai X, Li Y. The biological processes during wound healing. Regen Med 2021; 16(4): 373-390. doi: 10.2217/rme-2020-0066.
14. Vaidyanathan L. Growth factors in wound healing – a review. Biomed Pharmacol J 2021; 14 (3): 1469-1480. doi: https://dx.doi.org/10.13005/bpj/2249.
15. Johnson BZ, Stevenson AW, Prêle CM, Fear MW, Wood FM. The role of IL-6 in skin fibrosis and cutaneous wound healing. Biomedicines 2020; 8(5). doi: 10.3390/BIOMEDICINES8050101.
16. Jang DI, Lee AH, Shin HY, Song HR, Park JH, Kang TB, et al. The role of tumor necrosis factor alpha (TNF -α) in autoimmune disease and current TNF-α inhibitors in therapeutics. Vol. 22, International Journal of Molecular Sciences 2021; 22(5). doi: 10.3390/ijms22052719.

17. Xiao T, Yan Z, Xiao S, Xia Y. Proinflammatory cytokines regulate epidermal stem cells in wound epithelialization. Stem Cell Research and Therapy 2020; 11(1). doi: 10.1186/s13287-020-01755-y.
18. Gan M-S, Yang B, Fang D-L, Wu B-L. IL-1B can serve as a healing process and is a critical regulator of diabetic foot ulcer. Ann Transl Med 2022; 10(4): 1-11. doi: 10.21037/atm-22-75.
19. Russo B, Brembilla NC, Chizzolini C. Interplay between keratinocytes and fibroblasts : a systematic review providing a new angle for understanding skin fibrotic disorders. Front Immunol 2020; 11: 1-20. doi: 10.3389/fimmu.2020.00648.
20. Soliman AM, Barreda DR. Acute inflammation in tissue healing. International Journal of Molecular Sciences 2023; 24(1). doi: 10.3390/ijms24010641.
21. Bechara R, McGeachy MJ, Gaffen SL. The metabolism-modulating activity of IL-17 signaling in health and disease. Journal of Experimental Medicine 2021; 218(5). doi: 10.1084/jem.20202191.
22. Yahyapoor F, Sedaghat A, feizi A, Bagherniya M, Pahlavani N, Khadem-Rezaiyan M, et al. The effects of L-carnitine supplementation on inflammatory markers, clinical status, and 28 days mortality in critically ill patients: A double-blind, randomized, placebo-controlled trial. Clin Nutr ESPEN 2022; 49. doi: 10.1016/j.clnesp.2022.04.001.
23. Shahouzehi B, Fallah H. L-carnitine administration effects on AMPK, APPL1 and PPAR*γ* genes expression in the liver and serum adiponectin levels and homa-ir in type 2 diabetes rat model induced by STZ and nicotinamide. Ukr Biochem J 2020; 92(5): 33-40. doi. https://doi.org/10.15407/ubj92.05.033.
24. Chisty TTE, Sarif S, Jahan I, Ismail IN, Chowdhury FI, Siddiqua S, et al. Protective effects of L-carnitine on isoprenaline -induced heart and kidney dysfunctions: Modulation of inflammation and oxidative stress-related gene expression in rats. Heliyon 2024; 10(3). doi: https://doi.org/10.1016/j.heliyon.2024.e25057.
25. Baci D, Bruno A, Cascini C, Gallazi M, Mortara L, Sessa F. et al. Acetyl-L-Carnitine downregulates invasion (CXCR4/CXCL12, MMP-9) and angiogenesis (VEGF, CXCL8) pathways in prostate cancer cells: rationale for prevention and interception strategies. J Exp Clin Cancer Res 2019; 38(1). doi: 10.1186/s13046-019-1461-z.
26. Lin H, Jiang YC, Chen ZW, Zheng LL. Design, synthesis, and anti-inflammatory activity of indole-2-formamide benzimidazole[2,1-b]thiazole derivatives. RSC Adv 2024; 14: 16349-16357. doi. 10.1039/d4ra00557k.
27. Chiu YJ, Lin CH, Lin CY, Yang PN, Lo YS, Chen YC, et al. Investigating Therapeutic Effects of Indole Derivatives Targeting Inflammation and Oxidative Stress in Neurotoxin-Induced Cell and Mouse Models of Parkinson's Disease. Int J Mol Sci 2023; 24(3). doi: 10.3390/ijms24032642.
28. Honkisz-Orzechowska E, Łażewska D, Baran G, Kieć-Kononowicz K. Uncovering the power of GPR18 signalling: how RvD2 and other ligands could have the potential to modulate and resolve inflammation in various health disorders. Molecules 2024; 29(6). doi: 10.3390/molecules29061258.
29. Cao L, Wang Y, Wang Y, Lv F, Liu L, Li Z. Resolvin D2 suppresses NLRP3 inflammasome by promoting autophagy in macrophages. Exp Ther Med 2021; 22(5). doi: 10.3892/etm.2021.10656.
30. Bento AF, Claudino RF, Dutra RC, Marcon R, Calixto JB. Omega-3 Fatty Acid-Derived Mediators 17(R)-Hydroxy Docosahexaenoic Acid, Aspirin-Triggered Resolvin D1 and Resolvin D2 Prevent Experimental Colitis in Mice . J Immunol 2011; 187(4). doi: 10.4049/jimmunol.1101305.
31. Dort J, Orfi Z, Fabre P, Molina T, Conte TC, Greffard K, et al. Resolvin-D2 targets myogenic cells and improves muscle regeneration in Duchenne muscular dystrophy. Nat Commun 2021; 12(1). doi: 0.1038/s41467-021-26516-0.
32. Irvine HJ, Acharjee A, Wolcott Z, Ament Z, Hinson HE, Molyneaux BJ, et al. Hypoxanthine is a pharmacodynamic marker of ischemic brain edema modified by glibenclamide. Cell Reports Med 2022; 3 (6). doi: 10.1016/j.xcrm.2022.100654.
33. Yu T, Dong D, Guan J, Sun J, Guo M, Wang Q. Alprostadil attenuates LPS-induced cardiomyocyte injury by inhibiting the Wnt5a/JNK/NF-κB pathway. Herz 2020; 45 (S1): 130-138. doi: 10.1007/s00059-019-4837-0.
34. Yan X, Li Y, Choi YH, Wa C, Piao Y, Ye J, et al. Protective effect and mechanism of alprostadil in acute respiratory distress syndrome induced by oleic acid in rats. Med Sci Monit 2018; 24: 7186-7198. doi: 10.12659/MSM.909678.
35. Huang Q, Le Y, Li S, Bian Y. Signaling pathways and potential therapeutic targets in acute respiratory distress syndrome (ARDS). Respir Res 2024; 25(30): 1-32. doi: 10.1186/s12931-024-02678-5.
36. Baik B, Park S, Ji S, Yang W, Lee J. Effects of prostaglandin E1 and supplemental oxygen on the wound healing. J Wound Manag Res 2021;17(2): 108-114. doi: 10.22467/jwmr.2021.01613.
37. Issa NT, Stathias V, Schürer S, Dakshanamurthy S. Machine and deep learning approaches for cancer drug repurposing. Seminars in Cancer Biology 2021; 68. doi: 10.1016/j.semcancer.2019.12.011.
38. Sobolev VV, Tchepourina E, Korsunskaya IM, Geppe NA, Chebysheva SN, Soboleva AG, et al. The role of transcription factor PPAR-*γ* in the pathogenesis of psoriasis, skin Cells, and immune cells. Int J Mol Sci 2022; 23(17). doi: 10.3390/ijms23179708.
39. Briganti S, Mosca S, Di Nardo A, Flori E, Ottaviani M. New insights into the role of PPAR*γ* in skin physiopathology. Biomolecules 2024; 14(728):10–13. doi: https://doi.org/ 10.3390/biom14060728.
40. Ferdian PR, Nugroho HA, Phadmacanty NLPR, Handayani TH, Sugiartanti DD, Widyastuti A, et al. Acute oral toxicity of sunda porcupine's (*Hystrix javanica*, F. Cuvier 1823) quills crude extract on male Sprague Dawley rats using fixed dose method. AIP Conference Proceedings 2023; 2972 (1). doi: 10.1063/5.0183764.